Soft Matter

Spatiotemporal Control of Calcium Carbonate Nucleation Using Mechanical Deformations of Elastic Surfaces

Journal:	*Soft Matter*
Manuscript ID	SM-COM-04-2020-000734.R1
Article Type:	Communication
Date Submitted by the Author:	12-Jun-2020
Complete List of Authors:	Taylor, Jay; University of Nebraska-Lincoln, Chemistry Konda, Abhiteja; University of Nebraska-Lincoln, Chemistry Morin, Stephen; University of Nebraska-Lincoln, Chemistry

COMMUNICATION

Spatiotemporal Control of Calcium Carbonate Nucleation Using Mechanical Deformations of Elastic Surfaces

Jay M. Taylor,[a] Abhiteja Konda, [a] and Stephen A. Morin*[a,b]

Received 00th January 20xx,
Accepted 00th January 20xx

DOI: 10.1039/x0xx00000x

Biological systems generate crystalline material with properties and morphologies that cannot be duplicated using synthetic procedures. Developing strategies that mimic the control mechanisms found in nature would enhance the range of functional materials available for numerous technological applications. Herein, a biomimetic approach based on the mechano-dynamic chemistry of silicone surfaces was used to control the rate of heterogeneous $CaCO_3$ nucleation. Specifically, stretching the silicone surface redistributed functional groups tuning interfacial energy and thus the rate of $CaCO_3$ crystal formation, as predicted by classical nucleation rate laws. We extended this procedure using microrelief patterns to program surface strain fields to spatially control the location of nucleation. The strategies presented herein represent a fundamental departure from traditional bottom-up crystal engineering, where surfaces are chemically static, to them being active participants in the nucleation process controlling the outcome both spatially and temporally.

Introduction

Biomineralization encompasses a set of sophisticated strategies that living organisms employ to mineralize soft tissue to create rigid structural components (e.g., bone, teeth, etc.).[1, 2] The active spatial and temporal control over mineralization demonstrated in biology remains unrivalled by synthetic systems, which focus predominantly on the static control over crystallization (i.e., using steady state reactors or chemically stable substrates).[3, 4] We leverage the dynamic surface chemistry of elastic substrates to tune heterogeneous nucleation rates and for the first time, demonstrate synthetic systems capable of active spatial and temporal control over mineralization. Specifically, we developed soft, silicone substrates, with surface energies dependent on their mechanical state of strain and used these stimuli-responsive films to simultaneously tune the rate, location, and density of calcite (calcium carbonate, $CaCO_3$) nucleation. This synthetic approach, which focuses on dynamic surface properties, demonstrates an unprecedented level of control over crystal nucleation and establishes how surfaces with switchable chemical properties can accelerate or hinder chemical processes. We predict that these systems and the general strategies employed in their design, will influence the field of crystal engineering, which has been somewhat constrained by classical approaches that rely on static reaction conditions.

Biological organisms produce crystalline material that have unique and complicated structures, geometries, and compositions.[5, 6, 7] The sophistication of these crystals, which often have physical properties (i.e., mechanical, optical, and structural) that surpass what could be generated synthetically,[8-10] has driven the study of the mineralization pathways found in nature. Organisms use a multitude of mechanisms, many of which are still being elucidated, to form their crystalline material.[2] Many of these pathways originate inside cells and involve the use of intra/inter cellular vesicles to transport and concentrate ions as they are being delivered to mineralization sites.[2, 5, 10] Other pathways use proteins and organic matrices to help direct and stabilize nucleating crystals[11] or involve the use of 3D chemical micro-environments to template crystal formation.[6, 9]

Researchers, inspired by these crystallization mechanisms have focused on developing strategies that imitate these pathways (i.e., biomimetic strategies). For instance, researchers have explored the use of morphactants (e.g., amphiphiles, macromolecules, etc.) to change the shape of a growing crystal.[12] Understanding the interactions of biological macromolecules (i.e., DNA, peptides, and proteins), researchers have been able to redesign these biomacromolecules[13] to yield systems that demonstrate the programmed self-assembly of 3D structures that provide active mineralization scaffolds.[14]

Another popular biomimetic approach uses chemically modified surfaces to direct nucleation. A common strategy in

[a] Department of Chemistry, University of Nebraska-Lincoln, Lincoln, NE 68588.
[b] Nebraska Centre for Materials and Nanoscience, University of Nebraska-Lincoln, Lincoln, NE 68588; smorin2@unl.edu.
†Electronic Supplementary Information (ESI) available: [See ESI for information on materials and methods as well as details on FEA simulations]. See DOI: 10.1039/x0xx00000x

this area relies on the use of patterned self-assembled monolayers (SAMs) to control the nucleation rate, density, and orientation of growing crystals.[15] Other surface directed nucleation strategies include the use of engineered polymer surfaces,[16] biochemical matrices,[4, 17, 18] molecular layers assembled using Langmuir–Blodgett troughs,[3, 19] polyelectrolytes,[20 21] and block co-polymer films.[22] In all these reported demonstrations, the surface chemistry (i.e., functional group density, micropattern, and identity) was defined prior to nucleation. Previously, our lab has investigated how the mechanics of chemically modified soft silicone surfaces can be used to control the growth and adhesion of crystalline material.[23, 24] We hypothesized that these unique surfaces could be useful for the active control of crystal nucleation, and, in the present work, demonstrate that indeed soft silicone films with mechanically-tunable surface properties are able to tune crystal nucleation. We believe that these results represent a new approach to bottom-up crystal synthesis/fabrication that will inspire new biomimetic crystallization strategies.

In classical nucleation theory, the rate of heterogeneous nucleation is largely determined by the surface energies (γ) of the relevant interfaces (i.e., solution-crystal, solution-substrate, and substrate-crystal).[17, 20, 25] The steady-state nucleation rate (J_0) decreases exponentially as the thermodynamic barrier for nucleation (ΔG^*) increases,

$$J_0 = Ae^{-(\Delta G^*)/K_BT} \quad (1)$$

where A, is a pre-exponential factor specific to the crystal and surface, k_B is Boltzman's constant and T is absolute temperature. This thermodynamic barrier then scales cubically with the net surface energy of the system (γ_{net}) according to,

$$\Delta G^* = \frac{(F\omega^2\gamma_{net}^3)}{k_BT\sigma^2} \quad (2)$$

where F and h are geometric parameters, ω, is molar volume, σ, is supersaturation, and γ_{net} represents an interfacial energy relationship between the solution (L), surface (S), and crystal (C) defined by:

$$\gamma_{net} = \gamma_{LC} + h(\gamma_{SC} - \gamma_{SL}) \quad (3)$$

The ability to change this parameter quickly and easily would produce systems with active control over the thermodynamic barrier (ΔG^*), and thus the rate of nucleation (J_0), (Fig.1 A,B).

In this work, we focus on studying the crystallization behaviour of a model system, $CaCO_3$, which is well-studied because of its relevance to biomineralization. Previous studies of $CaCO_3$ nucleation reveal that at low supersaturations (σ = 5.0 – 6.0) substrates with lower surface energies (γ_S) nucleate $CaCO_3$ at higher rates compared with substrates of higher surface energies.[20, 26] In this case, substrates with lower surface energies interact more favourably with $CaCO_3$ compared to water, which helps to drive its formation on these surfaces. In our experiments, we used the low-surface-energy, soft silicone polydimethylsiloxane (PDMS; Sylgard 184) because its mechanics and chemistry are well understood and is compatible with aqueous mineralization reactions.

We prepared two types of PDMS films: "native" films that were prepared using manufacturer specifications (Fig. 1C), and "oxidized" films that were prepared by exposing native films to oxygen plasma followed by a mild chemical etching that removes the brittle surface silica layer formed during oxidation

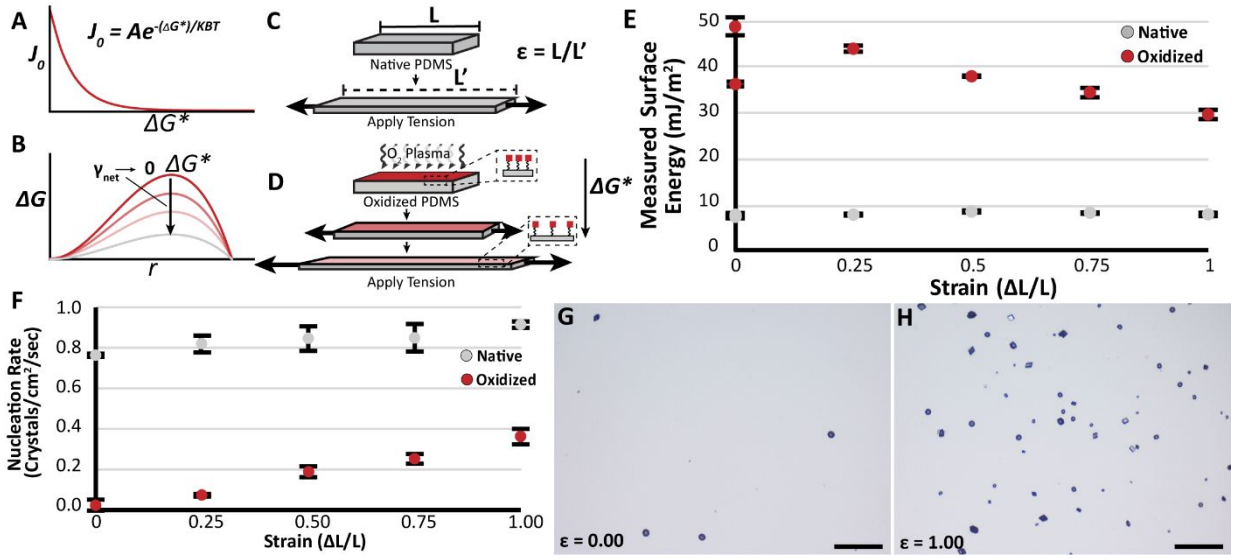

Fig. 1 Mechano-dynamic surfaces for modulation of heterogeneous nucleation. A) Theoretical plot of steady-state nucleation rate, J_0, versus the thermodynamic barrier to nucleation, ΔG^*. B) Series of theoretical curves of ΔG^* for decreasing surface energies, γ_{net}, at constant supersaturation (and thus critical nuclei radius, r^*). Oxidized films at increasing mechanical states of strain (red lines) approach ΔG* of the native PDMS films (grey line). C, D) Schematic illustrations of the change in ΔG^* associated with mechanical stress for the native PDMS films (panel C) and the oxidized PDMS films (panel D): ΔG^* remains constant for the native films but decreases for the oxidized films. E) E) Measurement of the specific surface energies of native and oxidized PDMS films using the Owens, Wendt, Rabel, and Kaelbel method at increasing strain states. F) Measurement of the steady-state nucleation rate of CaCO3 on native and oxidized PDMS films at increasing strain values (N = 3). G) Optical micrograph image showing a representative area of an oxidized film at ε = 0.00 after 40 minutes of growth and H) an oxidized film at ε = 1.00 after 40 minutes of growth (scale bars are 200 μm).

(Fig. 1D).[23] We then measured the specific surface energies of the two PDMS variants using established methods (see ESI for further details) at increasing mechanical states of strain (ε), defined by:

$$\varepsilon = \Delta L/L \qquad (4)$$

where L is the initial length of the substrate and ΔL is the change in length. The surface energy of the native films remained constant at close to 8 mN/m as we increased its strain, whereas, the surface energy of the oxidized films decreased from 50 mN/m to 25 mN/m as we increased the strain from ε = 0.0 to ε = 1.0 (Fig. 1E). We attribute this effect to a decrease in the density of silanol groups and a corresponding increase in the amount of unoxidized polymer at the surface associated with stretching the film. When tension is released from the substrate, the surface energy did not return to its initial value, which we attribute to monomer migration, as seen in previous studies.[27] Full reversibility of these systems can be achieved by re-oxidizing the surface or aided by storing the films in water.

We then measured the rate of $CaCO_3$ nucleation for these surfaces at increasing strain values and found that for the native surface nucleation rates remained relatively constant at 0.82 crystals·cm^{-2}·s^{-1} (Fig. 1F), consistent with our surface energy measurements, which also did not change upon stretching. On the oxidized substrates, however, we measured an increase in $CaCO_3$ nucleation rates by roughly an order of magnitude: 0.040 crystals·cm^{-2}·s^{-1} at ε = 0.0 increased to 0.37 crystals·cm^{-2}·s^{-1} at ε = 1.00 (Fig. 1F-H). These results agreed with the trend we expected from Eq. 1 and Eq. 2 which predict that decreases in the surface energy of the film (induced by mechanical tension in these studies) would lead to a corresponding increase in the nucleation rate of $CaCO_3$. In this study, the Ca^{2+} and CO_3^{2-} precursor solutions are premixed and then exposed to the chemically modified surfaces (this procedure is unlike in the popular ammonium diffusion method).[15] The solution-phase chemical equilibria of these precursor solutions supports the formation of neutrally charged $CaCO_{3(aq)}$ ion pairs and prenucleation clusters that interact favourably with native PDMS. We thus speculate that the observed difference in nucleation rates can be attributed to destabilization of the water/PDMS-OH interface associated with stretching oxidized films—strained films are more hydrophobic (Table S1) and thus interact more favourably with neutrally charged $CaCO_3$ ion pairs/prenucleation clusters than with water, therefore, replacing water with these species provides an increased thermodynamic driving force for heterogeneous nucleation. We also believe that the interaction between free Ca^{2+} ions and surface silanol groups will act to lower the concentration of these prenucleation clusters,[17, 20] and thus decrease the nucleation rate. Overall, these results demonstrate that the redistribution of silanol groups on the silicone surface creates a link between the mechanical state of strain and the $CaCO_3$ nucleation rate.

Next, we induced successive nucleation bursts at different strain states, enabling the production of bimodal crystal

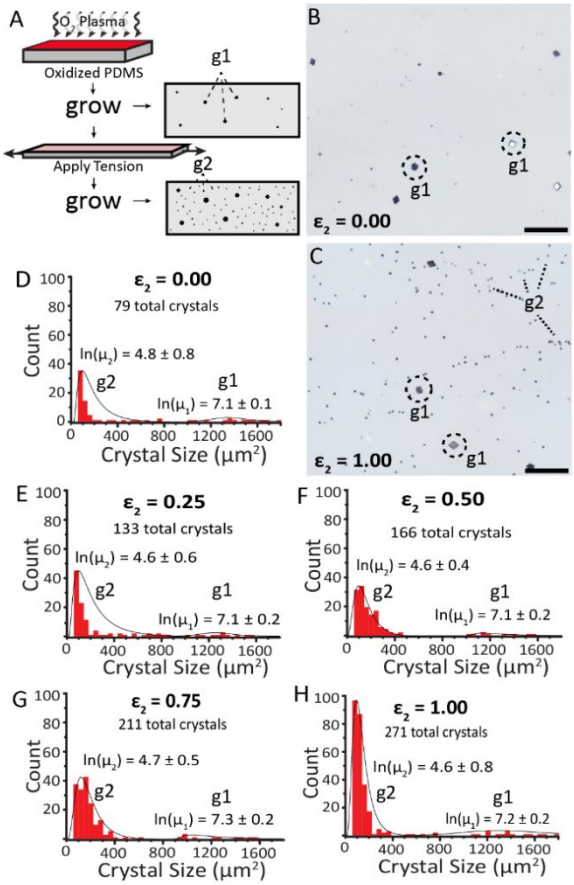

Fig. 2 Successive nucleation bursts on mechano-dynamic chemical surfaces. A) Schematic of the experimental design, where the first nucleation step occurs at a ε_1 = 0.00, resulting in *g1* crystals. The surface is stretched and subjected to a second nucleation step at ε_2, yielding *g2* crystals. B) Optical micrograph of film after second nucleation step where ε_2 = 0.00 (scale bar is 50 μm). C) Optical micrograph of film after second nucleation step, ε_2 = 1.00 (scale bar is 50 μm). D-H) Histograms comparing the populations of crystals after the second nucleation step, where the strain, ε_2, was systematically increased: D) ε_2 = 0.00, E) ε_2 = 0.25, F) ε_2 = 0.50, G) ε_2 = 0.75, H) ε_2 = 1.00.

populations (Fig. 2A). First, we grew a population of crystals (generation 1, *g1*) on an oxidized surface at ε_1 = 0.00 (t = 0 min.), and then, at a later time (t = 20 min.), a second population (generation 2, *g2*) of crystals were nucleated at a larger strain, ε_2. From t = 20 min. until t = 100 min. and until the end of the experiment, *g1* crystals will ripen, while *g2* crystals ripen for a comparatively shorter period. As a result, *g1* crystals will be larger than *g2* crystals, and, since *g2* crystals are nucleated on strained films that support higher nucleation rates, *g1* crystals will be lower in count than *g2* crystals. In accordance with this expectation, we observed bimodal population distributions in these experiments with a large population of small crystals (*g2*) and a small population of large crystals (*g1*) (Fig. 2B-C). Further, we found that by increasing the value of ε_2, we could increase the number of crystals nucleating during the second growth step, thus controlling the relative distribution of *g1* to *g2* crystals (Fig. 2D-H). Specifically, after a total growth time of 6000 seconds, the crystal density after the second growth step increased from 720 crystals/cm^2 at an ε_2 = 0.00 (Fig. 2B,D) to 2500 crystals/cm^2 area at an ε_2 = 1.00 (Fig. 2C,H). This trend agrees with the results from the single step growth experiments

(Fig. 1), though the observed nucleation rate during this second growth step was slightly larger than the expected growth rate for the targeted strain value. We attribute this difference to monomer migration over the course of the longer experiment, which acts to gradually lower the surface energy of the films. This demonstration shows that the mechano-dynamic surface properties of the silicon films can be used to rationally control the population distributions of crystals on the silicone's surface.

Next, we targeted the ability to spatially control the growth rate of $CaCO_3$ by rationally modulating surface strain fields using micro-relief patterns. In these experiments, we moulded our PDMS films to have two different thicknesses (Fig. 3A). Under tension, the thinner portions of the film would stretch more than the thicker portions, producing non-uniform stress fields (Fig. 3B). The deformation of these surfaces can be visualized under optical microscopy (Fig. S3) and modelled using finite element analysis simulations (Fig. 3C and Fig. S4). The micrographs and computational simulations reveal that when a macroscopic strain of 1.0 is exerted onto the film the thicker portions remain at a strain state close to zero, while the thinner portions deform to a strain state of close to 1.0.

We then tested the nucleation behaviour of these surfaces and hypothesized that when stretched the thinner regions of the surface would show an increase in crystallization density compared to the thicker portions of the substrate. In these experiments, we increased supersaturation slightly to generate higher overall crystal densities. We applied a mechanical strain of 1.00 to the film and then grew $CaCO_3$ on its surface. We found that the thinner portions of the film produced a crystal density of 11000 crystals/cm^2 (Fig. 3D-F), which is roughly 10 times greater than the thicker portions of the film which had a crystal density of 1000 crystals/cm^2 (Fig. 3D,E,G). At the higher supersaturations, the measured crystal density was larger than the density measured for lower supersaturations in prior experiments on flat films, but the trend of increasing crystal density by 10-fold between strains of ε = 0.00 and ε = 1.00 was consistent. Furthermore, when we did not apply strain to the film, we did not see a statistical difference in crystal density (Fig. 3H,I) between the thicker and thinner regions as both were close to the density of the films strained to ε = 0.00.

We further explored this concept by testing the nucleation behaviour of films where the thicker portions of the film were confined to islands. In this case, as strain is applied in one direction the thinner regions surrounding the island would respond anisotropically creating a more diverse strain field across the surface (Fig. 4A,B). As observed by optical microscopy images and finite element analysis simulations, when the film was stretched to a macroscopic strain state of ε = 1.0, the tops of the islands would experience a strain state close to 0.00, whereas the thinner regions parallel to the strain axis would deform to a strain state close to 1.0, and the regions perpendicular to the strain axis would deform to an intermittent strain value close ε = 0.60 due to the effects of Poison's compression (Fig. 4C, Fig. S5 and Fig. S6).

When we tested the nucleation behavior of these films, we observed crystal densities consistent with the mechanical state of strain experienced in each region. The crystal density was 1000 ± 30 crystals/cm^2 on the tops of the islands (Fig. 4D,E,G), 13500 ± 200 crystals/cm^2 across the thinner regions of the film parallel to the strain axis (Fig. 4D-F) and 7800 ± 300 crystals/cm^2 across the regions perpendicular to the strain axis (Fig. 4D,E,H). Also, when we applied no strain to the film, we observed no difference in nucleation rate (Fig. 4I,J). This demonstration shows even greater spatial control over nucleation, where crystal formation can be programmed by the resulting strain fields when the film is stretched. In these systems, we hypothesize that surface chemistry played the dominant role compared to any mass transport effects associated with the micropatterned film. The relative size of the features (500 µm) are much larger compared to the reported depletion zones for $CaCO_3$ (80 µm), and if we do not stretch the films the measured crystal densities between the thicker and thinner portions of the surface are statistically indifferent at 1000 crystals/cm^2.

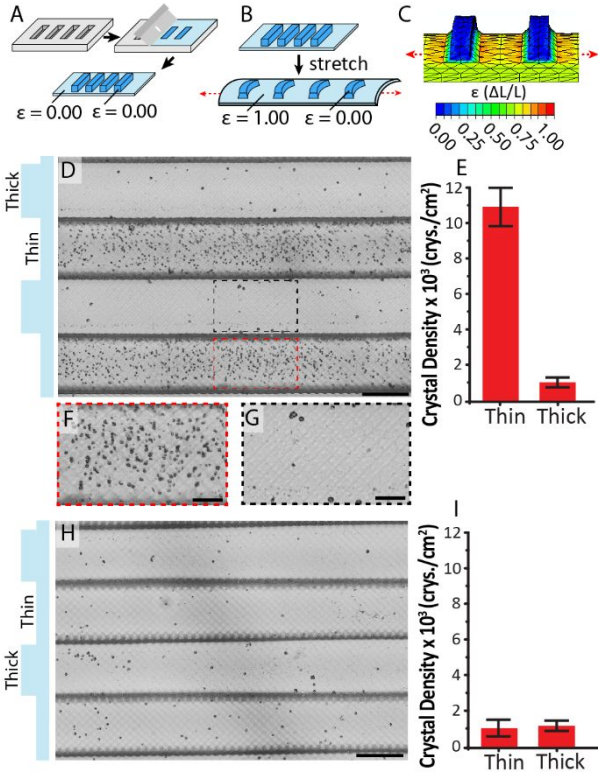

Fig. 3 Spatial control over $CaCO_3$ nucleation by heterogeneous strain fields programmed using microrelief patterns. A) Schematic illustration of the micro-moulding process used to create the microrelief pattern (which features thicker and thinner portions of PDMS). B) Schematic of the stretched film noting the differences in strain experienced at the thicker and thinner portions of PDMS. C) Finite element analysis simulations (FEA) of the moulded films when a strain of ε = 1.00 is applied to the film. D) Confocal microscope images of the surface of an oxidized film with microrelief pattern after nucleation at ε = 1.00 (scale 500 µm), and E) the corresponding histograms for crystal density on the thicker and thinner portions of the film (N = 4). F) Expansion of the red outlined area in D and G) expansion of the black outlined area in D (scale 50 µm). H) Confocal microscope image of an oxidized film with microrelief pattern after nucleation at ε = 0.00 (scale 500 µm). I) The corresponding histogram showing the crystal density on the thicker and thinner regions of the film.

Conclusions

In conclusion, we demonstrate a biomimetic approach based on the mechano-dynamic surface chemistry of silicone films to actively control the nucleation rates of $CaCO_3$. Through the application of

mechanical strain, we were able to redistribute surface functional groups, tuning interfacial energy, and thus the rate of heterogenous nucleation. Using this procedure, we were able to target specific nucleation densities using specific magnitudes of strain. In single-step growth experiments, we used this capability to generate populations of crystals at desired levels of surface coverage; in multi-step growth experiments, we used the mechano-dynamic properties of these surfaces to generate bimodal populations of surface crystals with predictable size/density relationships. By micro-molding relief structures, we programmed heterogenous strain fields which enabled spatial control of nucleation by tuning the localized strain magnitudes in specific nucleation zones. The results described in this work represent a departure from traditional bottom-up crystal engineering strategies where surfaces are treated as spectators and introduces a new strategy where the surface becomes an active participant in nucleation.

Herein we focused on $CaCO_3$ nucleation, but these principles can be readily applied to other crystal systems. We used silicone surfaces with only two functional groups, but these concepts can be extended using surfaces derivatized with other chemical moieties (i.e., those found more commonly in biological systems). The ability for surfaces to actively participate in mineralization reactions could lead to new methods to engineer crystal morphologies with enhanced mechanical, electrical, and optical properties. We also believe these results bring to the forefront a lesser explored parameter in stimuli responsive materials—the critical role of dynamic surface chemistry in controlling interfacial properties that could be critically important to various surface processes such as chemical reactivity and absorptivity, catalysis, wettability, and diffusion.

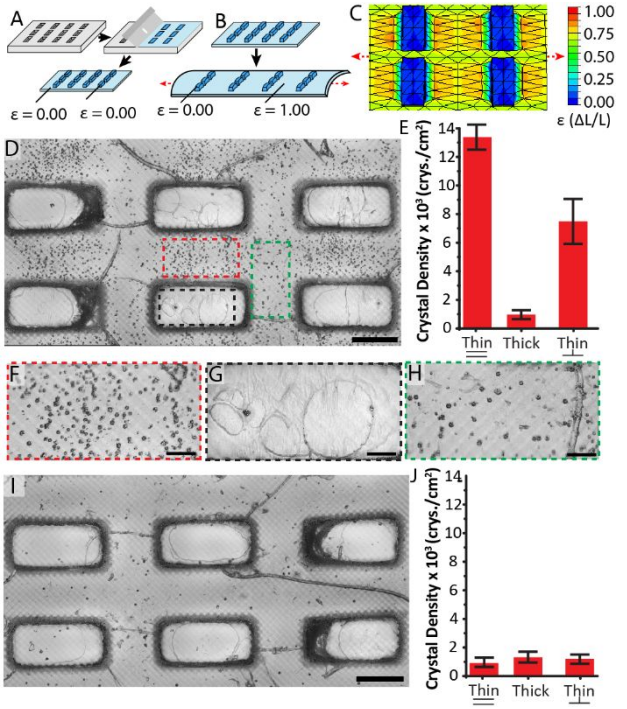

Fig. 4 Additional spatial control over $CaCO_3$ nucleation by heterogeneous strain fields programmed using microrelief patterns. A) Schematic illustration of the micro-moulding process used to create the microrelief pattern (which features thicker islands and thinner portions of PDMS). B) Schematic of the stretched film noting the differences in strain experienced at the thicker and thinner portions of PDMS. C) FEA simulations of the moulded films when a strain of $\varepsilon = 1.00$ is applied to the film. D) Confocal microscope images of the surface of an oxidized film with microrelief pattern after nucleation at $\varepsilon = 1.00$ (scale 500 μm), E) the corresponding histogram showing the crystal density on the thicker and thinner portions of the film with error bars showing standard deviation (N = 4). F) Expansion of the red outlined area in D), G) expansion of the black outline area in F) and H) expansion of the green outlined area in D. I) Confocal microscope image of an oxidized film with microrelief pattern after nucleation at ε = 0.00 (scale 500 μm). J) The corresponding histogram showing the crystal density on the thicker and thinner regions of the film.

Conflicts of interest

The authors declare no conflict of interest.

Acknowledgements

We thank the Dept. of Chemistry and the Nebraska Center for Materials and Nanoscience (NCMN) for start-up funds. S.A.M. thanks 3M for support through a Non-Tenured Faculty Award. This work was supported by the National Science Foundation under Grant No. 1555356. This research was performed in part at the NanoEngineering Research Core Facility and at the Nebraska Nanoscale Facility: National Nanotechnology Coordinated Infrastructure and the Nebraska Center for Materials and Nanoscience, which are supported by the National Science Foundation under Award ECCS:1542182, and the Nebraska Research Initiative.

Notes and references

1 A. Sahni, *J. Biosciences,* 2013, **38**, 925.
2 S. Weiner, L. Addadi, *Annu. Rev. Mater. Res.,* 2011, **41**, 21.
3 I. A. Aksay, M. Trau, S. Manne, I. Honma, N. Yao, L. Zhou, P. Fenter, P. M. Eisenberger, S. M. Gruner, *Science,* 1996, **273**, 892.
4 S. I. Stupp, P. V. Braun, *Science,* 1997, **277**, 1242.
5 E. Beniash, L. Addadi, S. Weiner, *J. Struct. Biol.,* 1999, **125**, 50.
6 N. Bouropoulos, S. Weiner, L. Addadi, *Chem. - Eur. J.,* 2001, **7**, 1881; Y. Levi-Kalisman, G. Falini, L. Addadi, S. Weiner, *J. Struct. Biol.,* 2001, **135**, 8.
7 J. M. Didymus, J. R. Young, S. Mann, *Proc. R. Soc. B,* 1994, **258**, 237.
8 R. Dillaman, S. Hequembourg, M. Gay, *J. Morphol.,* 2005, **263**, 356.
9 A. Levy-Lior, E. Shimoni, O. Schwartz, E. Gavish-Regev, D. Oron, G. Oxford, S. Weiner, L. Addadi, *Adv. Funct. Mater.,* 2010, **20**, 320.
10 S. Raz, S. Weiner, L. Addadi, *Adv. Mater.,* 2000, **12**, 38.
11 E. D. Sone, S. Weiner, L. Addadi, *Cryst. Growth Des.,* 2005, **5**, 2131; E. D. Sone, S. Weiner, L. Addadi, *J. Struct. Biol.,* 2007, **158**, 428.
12 S. Mann, *Angew. Chem., Int. Edit.,* 2000, **39**, 3393; C. M. Niemeyer, *Angew. Chem., Int. Edit.,* 2001, **40**, 4128; A. W. Xu, Y. R. Ma, H. Colfen, *J. Mater. Chem.,* 2007, **17**, 415.
13 H. G. Cui, M. J. Webber, S. I. Stupp, *Biopolymers,* 2010, **94**, 1; N. C. Seeman, H. F. Sleiman, *Nature Reviews Materials,* 2017, **3**, 17068; R. V. Ulijn, A. M. Smith, *Chem. Soc. Rev.,* 2008, **37**, 664.
14 X. G. Liu, F. Zhang, X. X. Jing, M. C. Pan, P. Liu, W. Li, B. W. Zhu, J. Li, H. Chen, L. H. Wang, J. P. Lin, Y. Liu, D. Y. Zhao, H. Yan, C. H. Fan, *Nature,* 2018, **559**, 593; C. B. Mao, D. J. Solis, B. D. Reiss, S. T. Kottmann, R. Y. Sweeney, A. Hayhurst, G. Georgiou, B. Iverson, A. M. Belcher, *Science,* 2004, **303**, 213; V. M. Yuwono, J. D. Hartgerink, *Langmuir,* 2007, **23**, 5033.
15 J. Aizenberg, A. J. Black, G. M. Whitesides, *Nature,* 1999, **398**, 495; J. Aizenberg, *Adv. Mater.,* 2004, **16**, 1295; J. Aizenberg, A. J. Black, G. H. Whitesides, *J. Am. Chem. Soc.,* 1999, **121**, 4500.
16 Y. Gan, F. B. Gu, D. M. Han, Z. H. Wang, G. S. Guo, *J Nanomater,* 2010; S. A. Morin, F. F. Amos, S. Jin, *J. Am. Chem. Soc.,* 2007, **129**, 13776.
17 P. J. M. Smeets, K. R. Cho, R. G. E. Kempen, N. A. J. M. Sommerdijk, J. J. De Yoreo, *Nat. Mater.,* 2015, **14**, 394.

18 N. A. J. M. Sommerdijk, G. de With, *Chem. Rev.,* 2008, **108**, 4499.
19 B. R. Heywood, S. Mann, *Adv. Mater.,* 1994, **6**, 9.
20 A. J. Giuffre, L. M. Hamm, N. Han, J. J. De Yoreo, P. M. Dove, *Proc. Natl. Acad. Sci. USA,* 2013, **110**, 9261.
21 Z. Y. He, W. J. Xie, Z. Q. Liu, G. M. Liu, Z. W. Wang, Y. Q. Gao, J. J. Wang, *Sci. Adv.,* 2016, **2**; L. Y. Wang, R. X. Yan, Z. Y. Hao, L. Wang, J. H. Zeng, J. Bao, X. Wang, Q. Peng, Y. D. Li, *Angew. Chem., Int. Edit.,* 2005, **44**, 6054.
22 S. H. Yu, H. Colfen, J. Hartmann, M. Antonietti, *Adv. Funct. Mater.,* 2002, **12**, 541; S. H. Yu, H. Colfen, *J. Mater. Chem.,* 2004, **14**, 2124.
23 J. J. Bowen, J. M. Taylor, C. P. Jurich, S. A. Morin, *Adv. Funct. Mater.,* 2015, **25**, 5520.
24 M. A. Rose, J. M. Taylor, S. A. Morin, *Chem. Mater.,* 2016, **28**, 8513; J. M. Taylor, C. Argyropoulos, S. A. Morin, *Adv. Mater.,* 2016, **28**, 2595.
25 I. V. Markov, *Crystal growth for beginners : fundamentals of nucleation, crystal growth and epitaxy*, World Scientific, Singapore ; River Edge, N.J. 2003; J. J. De Yoreo, P. G. Vekilov, *Rev Mineral Geochem,* 2003, **54**, 57.
26 Q. Hu, M. H. Nielsen, C. L. Freeman, L. M. Hamm, J. Tao, J. R. I. Lee, T. Y. J. Han, U. Becker, J. H. Harding, P. M. Dove, J. J. De Yoreo, *Faraday Discuss.,* 2012, **159**, 509.
27 K. Efimenko, J. Genzer, *Mater Res Soc Symp P,* 2002, **710**, 135; K. J. Regehr, M. Domenech, J. T. Koepsel, K. C. Carver, S. J. Ellison-Zelski, W. L. Murphy, L. A. Schuler, E. T. Alarid, D. J. Beebe, *Lab Chip,* 2009, **9**, 2132.

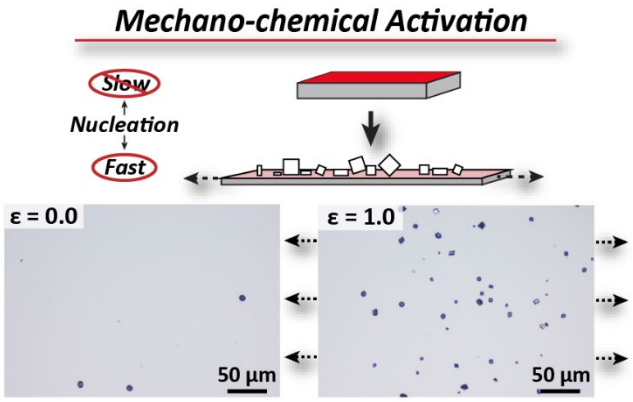

We demonstrate that chemically modified elastic surfaces can be used as active participants in crystal nucleation reactions. By stretching the elastomer, we redistribute functional groups that tunes interfacial energy in such a way that accelerates crystal nucleation.